Heliyon 10 (2024) e27907

Contents lists available at ScienceDirect

Heliyon

journal homepage: www.cell.com/heliyon

Research article

Computational investigation of turmeric phytochemicals targeting PTR1 enzyme of *Leishmania* species

Wasia Ullah [a], Wen-Feng Wu [b], Nosheen Malak [a], Nasreen Nasreen [a], Ayman A. Swelum [c], Liliana Aguilar Marcelino [d], Sadaf Niaz [a], Adil Khan [e,f,**], Mourad Ben Said [g,h,*], Chien-Chin Chen [i,j,k,l]

[a] *Department of Zoology, Abdul Wali Khan University Mardan, Mardan, 23200, Pakistan*
[b] *Department of Radiology, Ditmanson Medical Foundation Chia-Yi Christian Hospital, Chiayi, 600, Taiwan*
[c] *Department of Animal Production, College of Food and Agriculture Sciences, King Saud University, Riyadh, 1451, Saudi Arabia*
[d] *National Center for Disciplinary Research in Animal Health and Safety (INIFAP), Km 11 Federal Road Cuernavaca-Cuautla, 62550, Jiutepec, Morelos, Mexico*
[e] *Department of Zoology, Bacha Khan University Charsadda, Charsadda, 24420, Pakistan*
[f] *Department of Biology, Mount Allison University, Sackville, E4L 1G7, New Brunswick, Canada*
[g] *Laboratory of Microbiology, National School of Veterinary Medicine of Sidi Thabet, University of Manouba, Manouba, 2010, Tunisia*
[h] *Department of Basic Sciences, Higher Institute of Biotechnology of Sidi Thabet, University of Manouba, Manouba, 2010, Tunisia*
[i] *Department of Biotechnology and Bioindustry Sciences, College of Bioscience and Biotechnology, National Cheng Kung University, Tainan, 701, Taiwan*
[j] *Department of Pathology, Ditmanson Medical Foundation Chia-Yi Christian Hospital, Chiayi, 600, Taiwan*
[k] *Department of Cosmetic Science, Chia Nan University of Pharmacy and Science, Tainan, 717, Taiwan*
[l] *Ph.D. Program in Translational Medicine, Rong Hsing Research Center for Translational Medicine, National Chung Hsing University, Taichung, 40227, Taiwan*

ARTICLE INFO

Keywords:
In silico techniques
Parasite treatments
Neglected tropical diseases
Turmeric-derived phytochemicals
Leishmania pteridine reductase I (PTR1)
Molecular docking analysis
Binding affinities
Therapeutic potential
Rational drug design
Enzyme inhibition

ABSTRACT

In this study, we used *in silico* techniques to identify available parasite treatments, representing a promising therapeutic avenue. Building upon our computational initiatives aimed at discovering natural inhibitors for various target enzymes from parasites causing neglected tropical diseases (NTDs), we present novel findings on three turmeric-derived phytochemicals as inhibitors of *Leishmania* pteridine reductase I (PTR1) through *in silico* methodologies. PTR1, a crucial enzyme in the unique folate metabolism of trypanosomatid parasites, holds established therapeutic significance. Employing MOE software, a molecular docking analysis assesses the efficacy of turmeric phytochemicals against *Leishmania* PTR1. Validation of the docking protocol is confirmed with an RMSD value of 2. Post-docking, compounds displaying notable interactions with critical residues and binding affinities ranging between −6 and −8 kcal/mol are selected for interaction pattern exploration. Testing twelve turmeric phytochemicals, including curcumin, zingiberene, curcumol, curcumenol, eugenol, bisdemethoxycurcumin, tetrahydrocurcumin, tryethylcurcumin, turmerones, turmerin, demethoxycurcumin, and turmeronols, revealed

* Corresponding author. Laboratory of Microbiology, National School of Veterinary Medicine of Sidi Thabet, University of Manouba, Manouba, 2010, Tunisia.
** Corresponding author. Department of Zoology, Bacha Khan University Charsadda, Charsadda, 24420, Pakistan.
E-mail addresses: wasiullah.dir@gmail.com (W. Ullah), cych06454@gmail.com (W.-F. Wu), nosheenmalik496@gmail.com (N. Malak), nasreen@awkum.edu.pk (N. Nasreen), aswelum@ksu.edu.sa (A.A. Swelum), liliana@colpos.mx (L.A. Marcelino), sadaf@awkum.edu.pk (S. Niaz), dradilkhan@bkuc.edu.pk (A. Khan), bensaidmourad83@yahoo.fr (M. Ben Said), hlmarkc@gmail.com (C.-C. Chen).

https://doi.org/10.1016/j.heliyon.2024.e27907
Received 15 September 2023; Received in revised form 6 March 2024; Accepted 7 March 2024
Available online 16 March 2024

binding affinities ranging from −5.5 to −8 kcal/mol. Notably, curcumin, demethoxycurcumin, and bisdemethoxycurcumin exhibit binding affinities within −6.5 to −8 kcal/mol and establish substantial interactions with catalytic residues. These phytochemicals hold promise as lead structures for rational drug design targeting *Leishmania* spp. PTR in future applications. This work underscores the potential of these identified phytochemicals in the development of more effective inhibitors, demonstrating their relevance in addressing neglected tropical diseases caused by parasites.

1. Introduction

The utilization of *in silico* analysis aimed to identify the spectrum of currently available treatments for parasites, offering a method applicable for uncovering potential therapeutic avenues [1]. Especially in the context of neglected diseases, where the constraints of specialized drug development and limited commercial incentives impede substantial investment, repurposing drug candidates emerges as a refined facet of the *in silico* approach [2]. Curcumin, the extensively studied medicinal constituent comprising 0.3–5.4% of raw turmeric, has maintained a historical presence in Ayurvedic medicine due to its non-toxic nature and an array of therapeutic attributes encompassing analgesic, antioxidant, antibacterial, anti-carcinogenic, and anti-inflammatory properties [3]. Orally administered curcumin retains its structural integrity through the digestive tract, with a substantial fraction of 40–85 percent evading degradation. Metabolism primarily occurs within the liver and intestinal mucosa, processing the majority of absorbed flavonoid [4,5].

The molecular *in silico* docking technique is harnessed for establishing optimal ligand conformation and protein-ligand interactions, conventionally featuring a ligand and a receptor in tandem [6–8]. Prevalent tools and programs encompass Autodock Vina [9], Flex X [10], Autodock [11], and GOLD [12] among others. Previously, the emphasis has predominantly rested on the docking of two molecules through non-covalent associations encompassing electrostatic contacts, van der Waals interactions, and hydrogen bonds, as outlined by [10]. However, while not all drugs are designed for non-covalent interactions at the active site, many fall under the category of covalent pharmaceuticals [13]. The trend of non-covalent binding between ligands and receptors is gaining momentum.

Numerous successful docking techniques, such as those proposed in several studies [6,14,15] have arisen to predict the binding mode of non-covalent inhibitors. A significant computational method, molecular docking, extensively used to forecast ligand-receptor interactions [16], stands as a robust instrument in antileishmanial drug discovery. Synthetic analogues of natural chemicals have been found using *in silico* investigations, and new synthetic compounds with potential effectiveness against the parasite can be predicted for biosynthesis by docking studies [17]. Within the realm of *in silico* chemo-informatics research, the focus has gravitated toward comprehending the molecular underpinnings of human host-parasite interactions and forging novel drugs and vaccines against the ailment. A recent exploration engaged *in silico* methodologies to examine the potential of natural compounds derived from the Andean plant *Chrysophyllum cainito* as anti-leishmanial agents via molecular docking simulations [18]. The study unveiled several compounds with strong binding to a pivotal enzyme's active site in the *Leishmania* parasite, hinting at their viability as lead compounds for drug development.

Employing molecular dynamics simulations, an *in silico* study scrutinized the binding patterns of two innovative inhibitors targeting the crucial *Leishmania* enzyme, pteridine reductase 1 (PTR1). The inhibitors' ability to establish enduring interactions with the enzyme suggests their potential as exceptional candidates for pioneering Cutaneous Leishmaniasis (CL) drug development [19]. In the quest for prospective therapeutic targets in CL, a combined *in silico* analysis encompassing network-based and machine-learning methodologies was conducted to identify pivotal proteins and disease-associated pathways. The exploration encompassed multiple potential therapeutic targets, including enzymes within the *Leishmania* purine salvage pathway and proteins intricately linked to host immune responses [20].

Given the *Leishmania* parasite's unique capability to salvage pterins from the host, while the host lacks PTR1 activity and synthesizes pterin derivatives from GTP, the pteridine reductase 1 (PTR1) gene emerges as a paramount focus for therapeutic advancement [21]. Substantiated through numerous biochemical investigations, PTR1 is acknowledged as NADPH-dependent and functional in its tetrameric form [22–24]. This enzyme catalyzes the conversion of biopterin to H4 and H2 biopterin, along with the degradation of various folate forms, including 7, 8, and tetrahydrofolate. Notably, *Leishmania* PTR1 inhibition and potent antileishmanial activity are exhibited by dihydropyridines and 1-phenyl-4-glycosyl dihydropyridines [24,25]. The deletion of the PTR1 gene results in the death of insect stage promastigotes; however, this effect can be counteracted by providing reduced pterins, but not folates, suggesting that H4-biopterin plays a crucial function [26–28]. H4-biopterin's has recently been shown to play a part in controlling parasite differentiation. PTR1-deficient mutants exhibited reduced H4-biopterin levels, which caused the parasites within the sand fly vector to differentiate into the highly contagious metacyclic promastigote stage [29].

In this present investigation, we unveil the *in silico* discovery of diverse turmeric-derived phytochemicals as inhibitors of *Leishmania* pteridine reductase I (PTR1) through pharmacophore-based virtual screening and docking simulations.

2. Materials and methods

2.1. Protein selection and preparation

The *Leishmania* pteridine reductase 1 (PTR1) crystal structure was procured from the Protein Data Bank [https://www.rcsb.org]

under the PDB ID 1W0C, boasting a resolution of 2.60 Å. In this structure, each monomer of PTR1 accommodates the binding of 2,4,6-Triaminoquinazoline (TAQ), an analogue of methotrexate (MTX), within its active site. Therefore, this study necessitated only one chain, leading to the removal of the remaining two chains for expediency [30]. We analyzed the three-dimensional structure of PTR1, which was computationally and empirically predicted, in order to find solvent-exposed loops, flexible areas, and structurally conserved domains. PTR1's excess regions that were not directly connected to its ability to bind ligands or catalyze reactions were removed. This entailed cutting out flexible termini, solvent-exposed loops, and any other domains or regions that are not essential to the enzyme's operation. To make sure that the final protein structure was appropriate for *in Silico* analyses like molecular docking, molecular dynamics simulations, or structure-based drug design targeting PTR1, optimization was carried out based on modifying parameters i. e the size of the functionally relevant regions, the degree of pruning, and the criteria for excluding heteroatoms. The active site retained the NADPH co-factor, while surplus protein portions were pruned by excluding crystallographic water and extraneous heteroatoms, optimizing relevance to our study's goals. The crystal structures of PTR1 complexes exhibit large B-factors or missing portions of them, indicating great flexibility and the importance of entropy in binding [31]. MOE takes into account variables including steric conflicts, hydrogen bonding potential, and secondary structure preferences in order to forecast the most energetically favorable conformation for the missing residues using algorithms and energy minimization approaches. To address gaps in the protein sequence, the MOE software's (version 2022.02) loop modeler feature was employed, simulating missing residues. As adjustment of the protonation state of histidine influences protein structure, interaction and dynamics while addition of polar hydrogen play a crucial role in hydrogen binding which is a key interaction in maintaining the structure and stability of protein. That's why we adjusted protonation state of histidine and added polar hydrogen to ensure the significant interaction and the accuracy of the study. Employing the AMBER99 force field, energy minimization was conducted on the protein structure, further refining its suitability for subsequent analyses (Fig. 1).

2.2. Ligand preparation

Compounds including curcumin, zingiberence, curcumenol, curcumol, eugenol, bisdemethoxycurcumin, tetrahydrocurcumin, tryethylcurcumin, turmerin, turmerones, and demethoxycurcumin were sourced from PubChem and saved in Structure Data Files (SDF) format. The retrieved files were converted to PDB file format by using MOE software. To appropriately depict the pharmacophore, parameters such as hydrogen bond acceptor, hydrogen bond donor, hydrophobic group, lengths, and angles were adjusted. The energy minimization step employed the CHARMM (Chemistry at Harvard Macromolecular Mechanics Energy) force field [32] where the water molecules, heteroatoms, as well as any bound inhibitors in the protein–ligand complex were extracted since they were liable to influence the protein–ligand complex formation. Subsequently, based on the pH of the system, adjustment of protonation state was made and polar hydrogen atoms were added to facilitate compatibility with the docking process, rendering the compounds ready for the subsequent stages.

2.3. Molecular docking

Molecular docking, a cornerstone of structural molecular biology and computer-aided drug design, allowed us to predict ligand-protein interactions. The MOE software facilitated molecular docking analysis, enabling the simulation of binding modes between ligands and proteins with established 3D structures. Compounds having Post-docking analysis, exhibited binding affinities within the range of −6 to −8 kcal/mol were deliberately selected for further exploration due to their notable interactions with essential residues. The chosen binding affinity range (−6 to −8 kcal/mol) in the *in silico* analysis was important because it reflects a favorable range of energy values that were generally linked to strong binding interactions between a ligand and its target protein. This range was employed as a standard for locating potential lead compounds or promising therapies in molecular docking and virtual screening

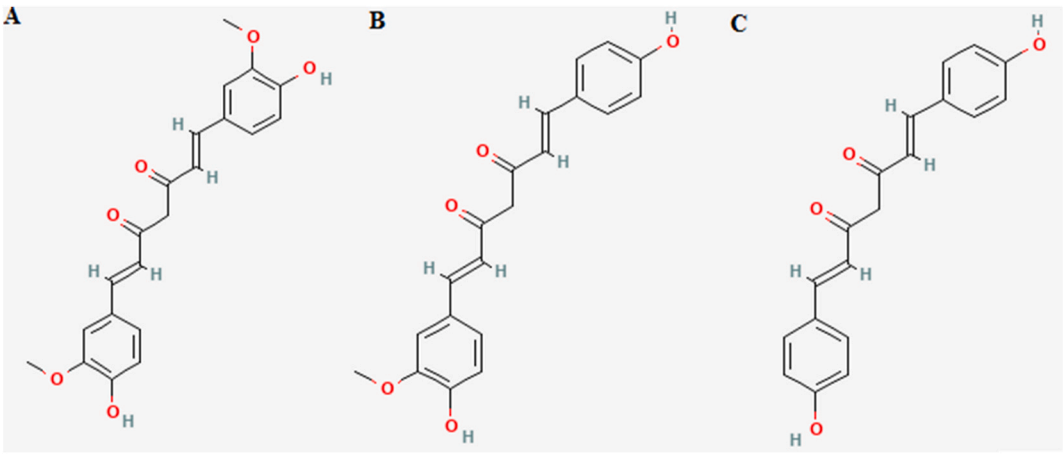

Fig. 1. Structure of curcumin (A), curcumin desmethoxycurcumin (B), and bisdemethoxycurcuminformatting (C).

investigations. A moderate to high binding affinity is represented by a range of −6 to −8 kcal/mol, suggesting that the ligand is likely to establish long-lasting interactions with the target protein. While validation docking methodology, its accuracy in predicting the binding mode and affinity of known ligands within a target protein's binding site was evaluated. Redocking experiments, in which the ligands were docked back into their native binding sites and the anticipated binding poses were compared with the empirically identified ones, are a popular method for benchmarking the docking procedure for validation. An effective method of evaluating the accuracy of the predicted binding postures is to use a threshold of 2 Å for the Root Mean Square Deviation (RMSD).

2.4. Protein hydrogen bonding analysis

Our inquiry into hydrogen bonds encompassed both hydrogen bonds and polar hydrogen bonds with predetermined bond lengths of 3.5 A°, culminating in a comprehensive assessment of the total count of hydrogen bond interactions.

2.5. ADMET properties calculation

The synthesis of *in silico* ADME/T (Absorption, Distribution, Metabolism, Excretion, and Toxicity) properties was achieved by harmonizing the capabilities of SwissADME and pkCSM, seamlessly integrated within an online platform. This amalgamation facilitated meticulous and comprehensive predictions, unraveling the intrinsic properties of the diverse phytochemicals derived from turmeric. The pivotal role of pkCSM server in determining ADMET properties and parameters, coupled with the execution of a drug design study via SwissADME, underscored the effectiveness of this approach.

2.6. Molecular dynamics simulations

Capitalizing on computational simulations, Molecular Dynamics (MD) emerged as a powerful technique to unravel the dynamic behavior of atoms or molecules within a virtual domain. Employing MD simulations, pivotal hydrogen bond interactions were unveiled, enhancing our grasp of protein docking and virtual screening methodologies. The iMODS server was harnessed in our study to orchestrate Molecular Dynamics simulations, granting insights into normal mode analysis and unearthing potential pathways within macromolecules or analogous structures.

The protein's topology was generated using the GROMOS96 force, while the ligand's topology followed the methodologies outlined by Refs. [32,33]. Subsequently, the compound-protein systems were solvated in a cubic box with periodic boundary conditions, employing the TIP3P water model. Neutralization was achieved by adding counterions, and energy clashes were rectified through energy minimization.

In the subsequent phase, the systems underwent equilibration in the NVT ensemble at 300 K and then in the NPT ensemble at 1 bar reference pressure. The final stage involved a 100 ns production run, maintaining constant temperature and pressure. Temperature control utilized the velocity-rescale thermostat, while pressure was regulated by the Parrinello-Rahman barostat.

3. Results

3.1. Molecular docking analysis

By efficiently excluding numerous non-binding candidates from the expansive chemical space, the synthesis and screening costs are substantially curtailed. The primary objective of this study was to leverage Docking-based virtual screening for the identification of novel prospective inhibitors of PTR1 from turmeric's repertoire of phytochemicals, encompassing curcumin, zingiberene, curcumol, curcumenol, and eugenol. Additionally, the roster comprises bisdemethoxycurcumin, tetrahydrocurcumin, tryethylcurcumin, turmerones, and demethoxycurcumin. Among the myriad strategies, molecular docking remains a robust and reliable approach for pinpointing the most potent inhibitor amid a vast array of chemicals. Employing this technique, the turmeric-derived phytochemicals are strategically docked within the active site of the target protein, specifically PTR1, in the quest for potential inhibitors [34].

Aided by the MOE software, a molecular docking simulation was conducted to visualize the interactive dynamics between PTR1 and the isolated compounds, furnishing a graphical representation of their binding interactions. Impressively, all compounds exhibited a marked preference for binding within the active site. The binding affinities of these compounds ranged from −5.5 to −8 kcal/mol. Notably, three compounds, namely curcumin, demethoxycurcumin, and bisdemethoxycurcumin (Fig. 1A–C), displayed binding affinities spanning −6.5 to −8 kcal/mol and demonstrated noteworthy interactions with catalytic residues. These compounds were selected for further in-depth investigation.

3.2. Molecular hydrogen bonds and hydrophobic interactions analysis

Evidenced by its impressive docking score of −7.82 kcal/mol and its favorable interaction profile with the PTR1 receptor, curcumin demonstrates substantial inhibitory activity. Illustratively depicted in Fig. 2A, five hydrogen bonds establish between curcumin molecules and the PTR1 receptor. Notably, the oxygen moieties of Ser 40 and Asp 181 in the PTR1 receptor form hydrogen bonds with the hydrogen components of curcumin at distances of 2.15 A° and 2.04 A°. Furthermore, the oxygen group of curcumin engages in hydrogen bonding with the hydrogen atoms of Arg 17, Leu 18, and His 38 in the PTR1 receptor, characterized by bond lengths of 2.59 A°, 2.93 A°, and 2.82 A°, respectively. Moreover, the PTR1 receptor interacts hydrophobically with Arg 39, Tyr 194, Pro 224, and Ser

227.

With a robust docking score of −7.5 kcal/mol, desmethoxycurcumin demonstrates a strong and favorable interaction with the PTR1 receptor. Particularly noteworthy are the three hydrogen bonds established between the molecule and the receptor. The hydrogen

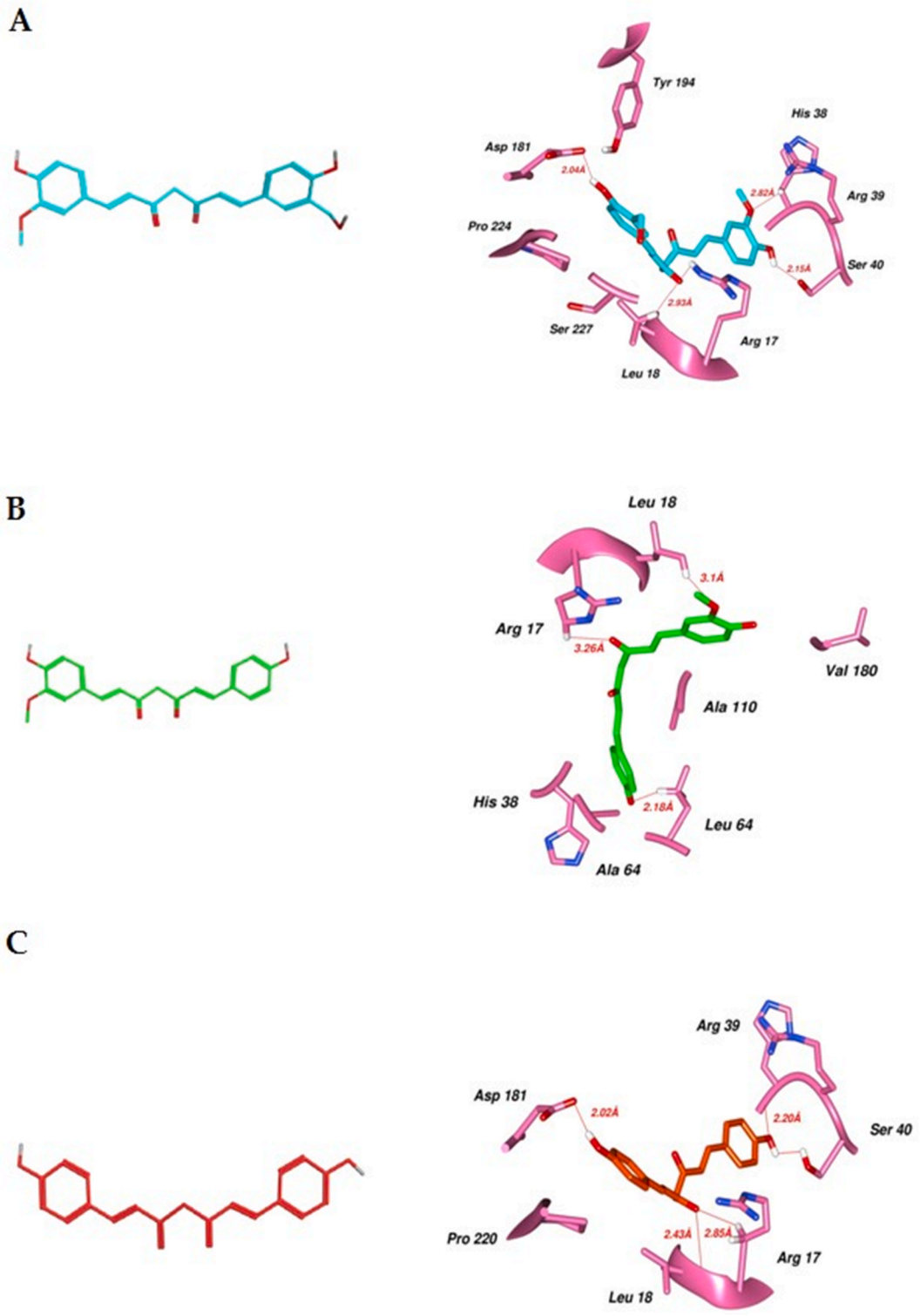

Fig. 2. Structure and interaction pattern with PTR1 receptor of Curcumin (A), demethoxycrcumin (B), and Bis demethoxycrcumini (C).

atoms of Leu 18, Arg 17, and Leu 64 amino acids and the oxygen atom of demethoxycurcumin are separated by distances of 3.26 A°, 3.10 A°, and 2.18 A°, respectively. Additionally, hydrophobic interactions ensue between the PTR1 receptor and His 38, Ala 110, and Val 180. The interaction pattern between desmethoxycurcumin and the PTR1 receptor is visualized in Fig. 2B.

Likewise, curcumin's interaction parallels that of bis-demethoxycurcumin, which boasts a binding score of −6.94 kcal/mol. Notably, bis-demethoxycurcumin generates five hydrogen bonds with specific amino acids of the PTR1 receptor – Arg 17, Leu 18, Arg 39, Ser 40, and Asp 181 – spanning distances of 2.85 A°, 2.43 A°, 2.20 A°, 3.12 A°, and 2.02 A°, respectively. Remarkably, a hydrogen bond involving hydrogen and oxygen atoms from both substances forms between the PTR1 receptor and bis-demethoxycurcumin. The interactions between PTR1 and bis-demethoxycurcumin are visually presented in Fig. 2C.

3.3. ADMET calculation results

To predict essential physicochemical attributes, absorption, distribution, metabolism, elimination, and pharmacokinetic properties of the synthesized compounds, the publicly accessible Swiss ADME web tool was harnessed in this investigation. The tool comprehensively evaluates six pivotal physicochemical properties encompassing lipophilicity, flexibility, saturation, polarity, solubility, and size [35].

Key physicochemical properties of compounds crucial in drug design include molecular weight, number of rotatable bonds, hydrogen bond acceptors (HBA), hydrogen bond donors (HBD), topological polar surface area (TPSA), Log P, Log S, and Violation. Molecular weight influences solubility, transport, and metabolism. Rotatable bonds signify molecular flexibility impacting binding affinity. HBA and HBD determine hydrogen bonding capacity, crucial for interactions with biological targets. TPSA correlates with hydrogen bond formation and influences permeability. Log P indicates compound lipophilicity, affecting absorption and distribution, while Log S reflects aqueous solubility, vital for bioavailability. Violation flags any rule violations, like Lipinski's Rule of Five, guiding drug-likeness assessment. These parameters collectively inform compound behavior and suitability for drug development.

The ADMET analysis conducted on the tailored compounds illuminated their physicochemical attributes, confirming adherence to Lipinski's rule of five (MW, iLOGP, HBAs, and HBDs), as delineated in Table 1. Encouragingly, none of the crafted compounds breached the stipulated parameters of the rule of five, signifying that their molecular weight, lipophilicity, count of hydrogen bond donors and acceptors, molecular polar surface area, number of rotatable bonds, and aromatic heavy atom count remained within permissible ranges. This collective adherence implies that the compounds possess favorable pharmacokinetic traits. Thus, the utilization of Swiss ADME in this *in silico* analysis underscores the promising pharmacokinetic profiles exhibited by the designed compounds. This augments their potential as valuable contenders for subsequent exploration and eventual clinical trials.

In the preliminary phases of drug exploration, the selection of compounds devoid of carcinogenic and hepatotoxic traits holds paramount significance [28]. The scope of toxicity assessment (ADMET, with the "T" representing Toxicity) encompasses the prediction of mutagenicity and carcinogenicity, among other factors. Among the endpoints employed for toxicity evaluation are Ames toxicity, hepatotoxicity, and oral rat acute toxicity (LD50). The LD50 value and the categorization of chemical toxicity according to the Globally Harmonized System (GHS) contribute to gauging the extent of substance toxicity. The pertinent ADMET parameters are tabulated in Table 2. Absorption parameters predict compound absorption in biological systems. Water Solubility (log mol/L) correlates with absorption; higher values suggest better absorption. Caco2 Permeability (log Papp, cm/s) indicates intestinal absorption potential; higher values imply better absorption. Intestinal Absorption (human) (%) predicts absorption percentage through intestines. Skin Permeability (log Kp) (cm/s) assesses skin permeability; lower values indicate better permeability (Table 3).

The ADMET attributes of turmeric-derived phytochemicals unveil robust solubility, indicative of favorable absorption and efficient elimination through the urinary tract. Impressively elevated Human Intestinal Absorption (HIA) values denote a greater than 90% likelihood of intestinal absorption for all three compounds. Calculated using the log of the apparent permeability coefficient (log Papp) in the Caco-2 cell line, recognized as an in vitro model of the human intestinal mucosa, drug absorption is often determined. On the pkCSM webserver, a chemical achieves high Caco-2 permeability if its log Papp value exceeds 0.90 cm/s. As detailed in Table 2, all compounds, barring curcumin (0.847 cm/s), exhibit elevated Caco-2 permeability.

In the context of effective drug delivery, skin permeability (log Kp) holds critical significance, particularly in the domain of transdermal drug administration development. The recommended log Kp value stands above −2.5 cm/h [36]. Impressively, calculated log Kp values for all compounds fall within the range of −2.763 to −3.017 cm/h, affirming their substantial potential for skin penetration.

3.4. Distribution and excretion assessment

Distribution parameters assess compound distribution in the body. VDss (human) (log L/kg) predicts volume of distribution at

Table 1
Post docking analysis and E-value of the best interaction of Curcumin, Demethoxycurcumin and Bis demethoxycurcumin compounds with PTRI protein..

Compound name	E-value	H-bond	Bonding residues
Curcumin	−7.82	5	Ser 40, Asp 181, Arg 16, Leu 18, His 38
Demethoxycurcumin	−7.5	3	Leu 18, Arg 17, Leu 64
Bis Demethoxycurcumin	−6.74	5	Arg 17, Leu 18, Arg 39, Ser 40, and Asp 181

Table 2
In silico calculated physicochemical properties of turmeric phytochemicals..

Compoundnames	Molecular weight	Num. Rotatable bonds	HBA	HBD	TPSA	Log *P*	Log *S*	Violation	Swiss Bar
Curcumin	368.38 g/mol	8	6	2	93.06 Å^2	3.27	−3.94	0	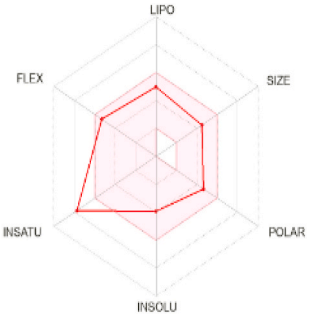
Demethoxycurcumin	338.35 g/mol	7	5	2	83.83 Å^2	2.78	−3.92	0	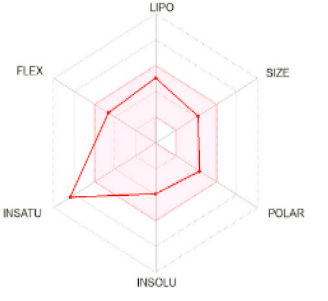
Bis demethoxycurcumin	308.33 g/mol	6	4	2	74.60 Å^2	1.75	−3.80	0	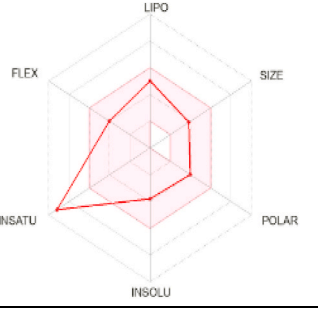

Table 3
Pharmacokinetic profile and toxicity prediction of turmeric phytochemicals..

Parameters	Curcumin	Demethoxycurcumin	Bis demethoxycurcumini
ABSORPTION Water solubility (log mol/L)	−5.157	−3.387	−4.618
Caco2 permeability (log Papp, cm/s)	0.847	1.1	0.915
Intestinal absorption (human) (%)	91.365	91.027	97.244
Skin Permeability (log Kp) (cm/s)	−3.054	−2.763	−3.017
DISTRIBUTION VDss (human) (log L/kg)	0.256	0.097	0.369
BBB permeability (log BB)	−0.406	−0.229	−0.029
METABOLISM CYP2D6 substrate	No	No	No
CYP3A4 substrate	Yes	Yes	No
EXCRETION Total Clearance	0.763	0.039	0.531
Renal OCT2 substrate	No	No	No
TOXICITY AMES toxicity	No	No	No
Oral Rat Acute Toxicity (LD50) (mol/kg)	2.983	2.13	2.689
Hepatotoxicity	No	No	No

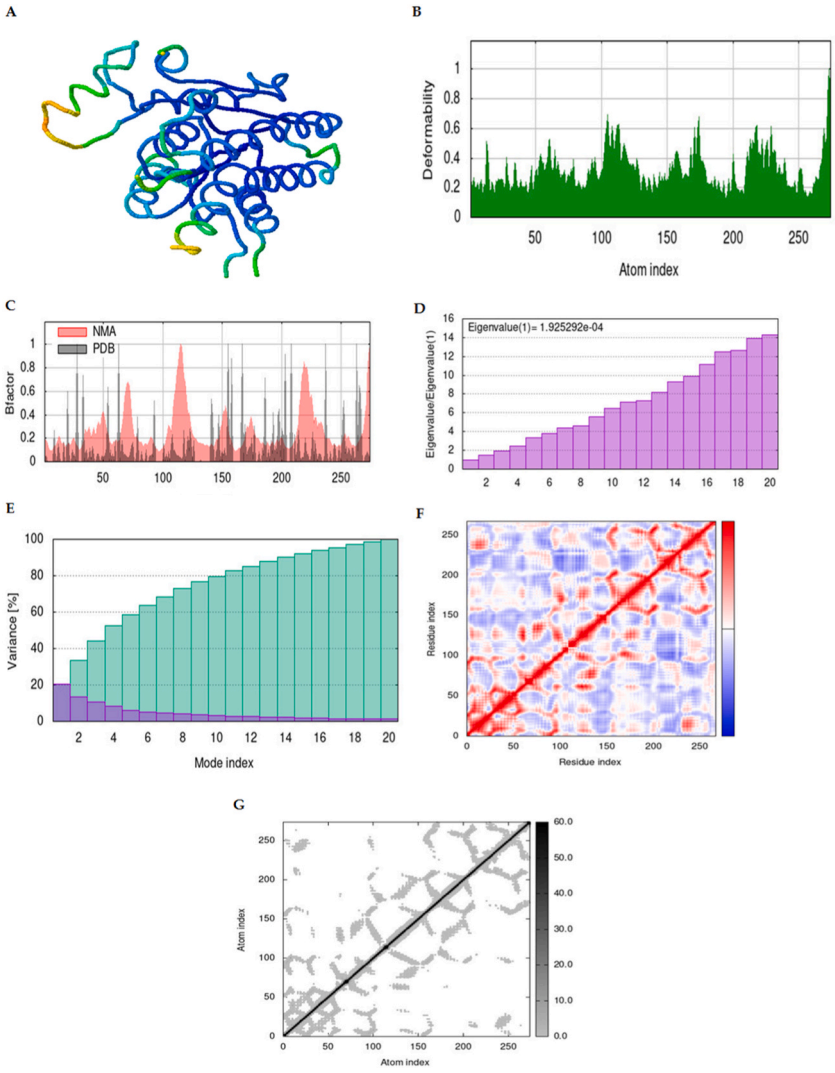

Fig. 3. Findings of molecular dynamics (MD) simulations for the complex formed between our ligand and the PTR1 receptor. Image A displays the docked complex of the protein and ligand. Image B illustrates the deformability graph, while Image D shows the eigenvalue of the complex. Image E represents the variance plot, and Image G presents the elastic map of our docked complex. Furthermore, Image F showcases the covariance map, and Image C displays the B-Factor graph.

steady state, reflecting extent of distribution. BBB Permeability (log BB) predicts blood-brain barrier permeability; lower values imply reduced CNS effects. In gauging a drug's distribution within the body, the volume of distribution at steady state (VDss) and the blood-brain barrier (BBB) stand as pivotal considerations. A higher VDss value denotes heightened drug delivery to tissues as opposed to plasma. Notably, a VDss value exceeding 0.45 is indicative of favorable distribution [37,32]. In this study, the VDss values of all compounds fall within the range of 0.097–0.369.

Regarding the BBB, a pivotal determinant of a drug's ability to penetrate the brain while minimizing undesirable effects, a molecule showcases effective permeability across the barrier when its log BB value surpasses 0.3. Given that the examined phytochemicals possess log BB values below 0.3, their capacity to penetrate the blood-brain barrier remains constrained [34]. Metabolism parameters indicate compound metabolism. CYP2D6 and CYP3A4 are enzymes involved in the metabolism of various drugs and xenobiotics in the human body. Understanding whether a compound is metabolized by these enzymes is crucial for predicting potential drug-drug interactions, and determining dosing regimens. Metabolism analysis indicates that all compounds are not metabolized by CYP2D6, while Curcumin and Demethoxycurcumin are substrates for CYP3A4, suggesting potential metabolism by this enzyme. Bis demethoxycurcumini is not a substrate for CYP3A4, implying limited metabolism via this pathway.

Excretion parameters determine compound clearance. Total Clearance predicts clearance rate; higher values imply faster clearance. Renal OCT2 Substrate indicates substrate status for the transporter OCT2, relevant for renal excretion.

In the domain of excretion parameters, encompassing total clearance and interaction with the organic cation transporter 2 (OCT2), the lower segment of Table 2 furnishes relevant details. OCT2, a crucial protein transporter, plays a pivotal role in the renal uptake, disposition, and clearance of pharmacological entities. The overall clearance is closely linked with renal OCT2 activity, offering insights not only into compound clearance but also potential contraindications [38]. Toxicity parameters assess compound safety. AMES Toxicity predicts mutagenicity; a positive result indicates potential mutagenicity. Oral Rat Acute Toxicity (LD50) predicts acute toxicity in rats; LD50 is the dose at which 50% die. Hepatotoxicity indicates potential liver toxicity. Remarkably, the pKCSM projections indicate that all phytochemicals examined in this study are non-substrates for OCT2. The toxicity analyses collectively demonstrate the non-mutagenic and non-hepatotoxic nature of all compounds.

The integration of SwissADME and pkCSM within the online platform was achieved through careful coordination of their APIs (Application Programming Interfaces) to seamlessly combine their predictive capabilities. By giving consumers access to an all-inclusive set of drug discovery tools through a single interface, this integration increases the efficacy of the method. The platform simplifies the drug discovery process, encourages effective data analysis, and boosts confidence in compound assessment by combining various predictions covering physicochemical properties, pharmacokinetics, toxicity, and protein-ligand interactions. This ultimately speeds up drug development efforts.

3.5. Molecular dynamics simulations

The rationale behind selecting the iMODS server for conducting Molecular Dynamics simulations lies in its robust capabilities for normal mode analysis and exploration of potential pathways in biomolecular systems. In order to examine the collective motions of proteins and nucleic acids and get important insights into their dynamics and function, iMODS provides sophisticated algorithms. Researchers may quickly and effectively find low-frequency normal modes linked to large-scale motions, including conformational changes or domain motions, by using iMODS. Additionally, iMODS facilitates the identification of potential allosteric communication pathways within biomolecules, aiding in the understanding of complex biological processes. All things considered, iMODS is an effective method for clarifying the dynamic behavior of biomolecular systems and revealing crucial functional pathways.

The outcomes of Molecular Dynamics (MD) simulations are elucidated through Fig. 3. From the ensemble of docked complexes, the MD simulation selected the optimal one – the ligand and PTR1 receptor bound with Curcumin. With a focus on studying large-scale mobility, B-factor, and stability of the molecules, normal mode analysis was conducted. The IMOD server facilitated the evaluation of internal coordinates pertaining to protein-ligand structural interactions. Computation of B-Factor, structural deformity, and eigenvalues followed suit. Fig. 3 portrays Image A, depicting the docked complex of the protein and ligand, while Image B unveils the deformability graph, spotlighting regions marked by elevated deformability peaks.

Image C delineates the B-Factor graph, portraying the main-chain deformability of the molecule at each residue. Correspondingly, Image D provides insight into the eigenvalue associated with each normal mode, serving as an indicator of motion stiffness. Lower eigenvalues correlate with increased deformability. Within our docked complex, the eigenvalue registered at 1.925292e-04. Image E visualizes the variance plot, characterized by individual variances in red and cumulative variance in green. Further, Image F elucidates the covariance map, disclosing correlated motion in red, uncorrelated motion in white, and anti-correlated motion in blue between residue pairs.

Image G extends the understanding with the presentation of the elastic map, each dot signifying a spring connecting atom pairs. The color code reflects stiffness. The MD inquiry unveiled substantial deformability within our complex, accompanied by a reasonably low eigenvalue, indicative of facile deformation. The variance map showcased higher cumulative variances in contrast to individual variances, while the elastic network map furnished gratifying outcomes.

Molecular dynamics (MD) simulation proves to be a valuable tool for investigating both internal and external motions, along with conformational changes concerning the average positions of all atoms. Consequently, a simulation study was conducted to elucidate the time-dependent motion of the chosen ligand within the protein's binding pocket. The analysis toolkit for molecular dynamics simulations encompasses root mean square deviation (RMSD) and root mean square fluctuation (RMSF).

In essence, RMSD provides insights into overall stability by quantifying divergence from the initial structure. In the ligand-free state (apo system), the target protein exhibited fluctuations up to 60 ns, stabilized until 80 ns, with noticeable backbone variations, as

showed in Fig. 4A. The complex, on the other hand, demonstrated significant stability despite fluctuations, as illustrated in Fig. 4A. Initially, the compound experienced fluctuations between 20 and 50 ns, followed by a more stable period between 60 and 80 ns, ultimately reaching a relatively stable RMSD towards the end of the MD simulation.

RMSF, representing the average displacement of each residue post-ligand binding, was utilized to assess the dynamics of residue side chains over time for both the apo system and the complex (Fig. 4B). Another crucial parameter, the radius of gyration (Rg), serves as a fundamental indicator of the overall size of the chain molecule, evaluating its compactness and flexibility within a biological

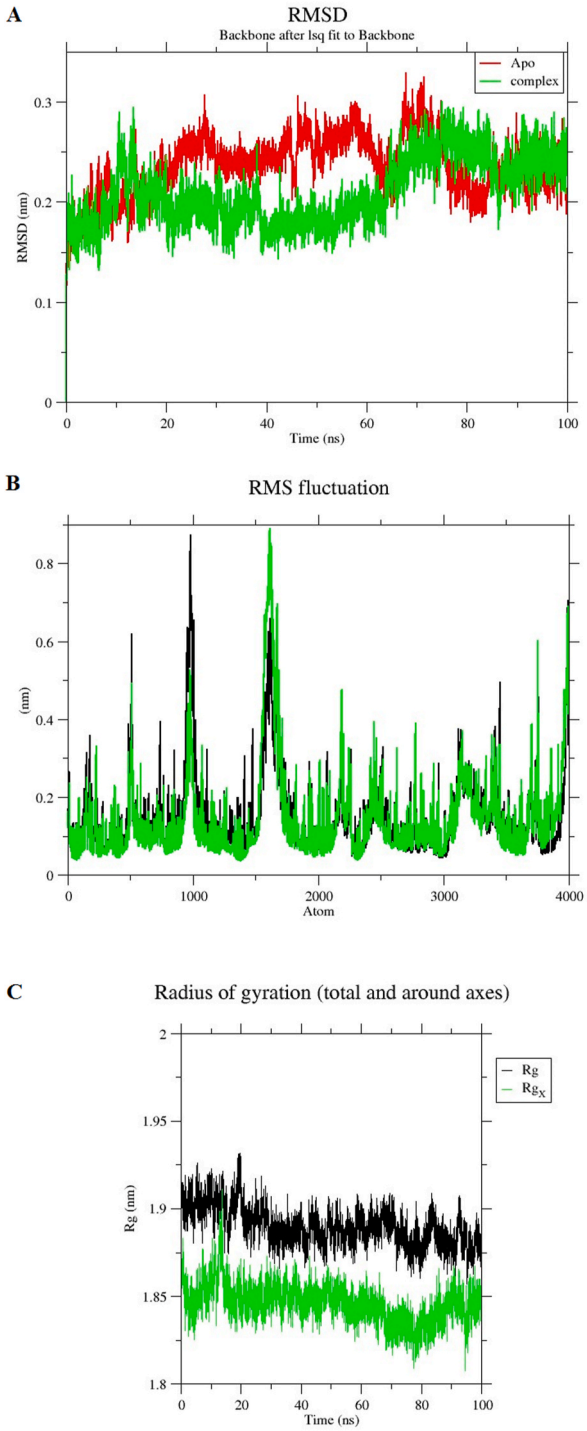

Fig. 4. Comparative analysis of Apo protein and ligand-based complexes: RMSD (A), RMSF (B), and Rg plots (C).

environment. Lower Rg values indicate a more rigid structure during the simulation. The Rg of the particle over time (Fig. 4C) showcases its mass distribution around the center of rotation. The generally stable Rg around 1.9 nm suggests a compact structure, with a slight dip to 1.85 nm around 40 ns, indicating a potential temporary tightening of the particle's configuration. Importantly, the Rg values for both the total particle and its rotation around a specific axis (R8x) closely coincide, suggesting a relatively symmetrical shape, as presented in Fig. 4C.

4. Discussion

Through the use of docking-based virtual screening, this study explored the potential of various phytochemicals from turmeric, including curcumin, zingiberene, curcumenol, curcumol, eugenol, bisdemethoxycurcumin, tetrahydrocurcumin, tryethylcurcumin, turmerin, turmerones, and turmeronols, as inhibitors of PTR1. Strikingly, all these compounds exhibited a strong tendency to selectively bind within the active site. Their binding affinities ranged from −5.5 kcal/mol to −8 kcal/mol. Significantly, three compounds, namely curcumin, demethoxycurcumin, and bisdemethoxycrcumin, stood out for their substantial interactions with catalytic residues and binding affinities falling between −6.5 and −8 kcal/mol. These compounds were singled out for further investigation, underscoring their potential as valuable subjects for in-depth PTR1 inhibition studies.

Indeed, other investigations have contributed to our understanding of the antileishmanial properties inherent in turmeric's compounds. The molecular interactions revealed in our study showcase how Curcumin establishes a network of five hydrogen bonds with the PTR1 receptor, further underscoring its potential as an inhibitor. Similarly, Demethoxycurcumin's interaction with PTR1 involves three hydrogen bonds, while Bis demethoxycurcumin mirrors this pattern with five hydrogen bonds. These interactions shed light on the intricate binding mechanisms underlying the compounds' potential antileishmanial activity.

Turning to clinical insights, the effectiveness of turmeric constituents against leishmaniasis has been documented. The utilization of a herbal remedy, containing C. longa as an active component, showcased encouraging outcomes. Among patients afflicted with cutaneous leishmaniasis, the administration of this plant juice combination resulted in a healing rate of around 40%, surpassing the 32.71% curative rate observed with the exclusive use of Meglumine antimonate [39].

Moreover, deeper investigations spotlighted the potency of curcumin against severe leishmaniasis. Notably, concentrations as low as 2 mg/L within the complete turmeric extract exhibited rapid eradication of promastigotes within a mere 88 h, in contrast to the 0.2 mg/L concentration [40]. This finding not only highlights curcumin's efficacy at relatively lower doses but also underscores its quantitative superiority over Glycyrrhiza glabra (liquorice). Exploring combined therapies [41], proposed the synergistic potential of Miltefosine and Nano curcumin as a promising approach for diseases linked to leishmaniasis. This combined treatment approach not only targeted promastigotes and amastigotes but also elevated phagocytic activity and reactive oxygen and nitrogen species production. These findings collectively deepen our appreciation for the multifaceted potential of turmeric's compounds. They evoke parallels with other natural sources, such as Jugans regia, where similar antibacterial properties, notably cyclobutanol, were uncovered [42].

In this current study, the focus of our *in silico* analysis was directed toward the PTR1 gene. This gene has garnered substantial attention in prior investigations involving molecular docking techniques. The availability of the complete genome sequence has indeed broadened the scope of identifying potential therapeutic targets [43]. Of note, PTR1 stands as a pivotal enzyme under scrutiny as a prospective therapeutic target. Research by Refs. [44–46] collectively highlighted the gene's indispensability, as deletion of the PTR1 gene proved to be lethal for *Leishmania*'s promastigote stage. The pivotal role of unconjugated pteridines further emerged, with studies indicating that PTR1 synthesis effectively circumvented anti-pteridine inhibition, providing a crucial metabolic bypass for DHFR-TS inhibition [43–45].

The well-established 3D structure of PTR1 in the parasite context serves as a robust foundation for the development of targeted inhibitors with selectivity for the parasite [47,48]. Incorporating covalent molecule docking into computer-aided drug design strategies allows for the characterization of covalent bonds between biological targets and inhibitors, enriching our understanding of interactions [49]. Interestingly, our study suggests the likelihood of robust electrochemical interactions between curcumin, demethoxycurcumin, bisdemethoxycurcumin, and the PTR1 protein.

Amidst the diverse array of twelve phytochemicals in turmeric, it's noteworthy that only three, curcumin, bisdemethoxycurcumin, and demethoxycurcumin, exhibited tangible health benefits according to our findings. This observation underscores the potential significance of these compounds in the context of therapeutic applications.

5. Conclusion

In this study, we harnessed the power of *in silico* screening encompassing pharmacophore-based virtual screening and docking simulations to uncover a novel class of *Leishmania* PTR1 inhibitors from a diverse pool of naturally occurring compounds. Notably, among the twelve phytochemicals present in turmeric, three emerged as particularly promising, highlighting the efficacy of the virtual screening methodology driven by pharmacophore and docking approaches. Our exploration of docking simulation results unveiled a consistent pattern of interactions and binding modes between the selected inhibitors and PTR1's substrate binding site. Of significance was the recognition of interactions with the crucial co-substrate, NADPH. To validate this hypothesis, further investigations are warranted, including a comprehensive examination of inhibitory kinetics. The inhibitors uncovered through this research hold significant potential as foundational stepping stones for the future prediction and development of more potent PTR1 inhibitors. As we continue to unravel the intricacies of these interactions, this work lays the groundwork for advancing our understanding of parasite-targeted therapeutic interventions in the ongoing battle against *Leishmania* infections.

Funding

No funding is applied for this current project.

Data availability statement

The data that support the findings of this study are available from the corresponding author upon request.

CRediT authorship contribution statement

Wasia Ullah: Writing – original draft, Visualization, Methodology, Conceptualization. **Wen-Feng Wu:** Writing – review & editing, Data curation, Conceptualization. **Nosheen Malak:** Writing – original draft, Software, Investigation. **Nasreen Nasreen:** Supervision. **Ayman A. Swelum:** Writing – review & editing, Funding acquisition. **Liliana Aguilar Marcelino:** Resources, Data curation. **Sadaf Niaz:** Supervision, Formal analysis. **Adil Khan:** Writing – original draft, Validation, Supervision, Project administration, Investigation. **Mourad Ben Said:** Writing – review & editing, Visualization, Validation, Formal analysis, Data curation. **Chien-Chin Chen:** Resources, Project administration.

Declaration of competing interest

The authors declare that they have no known competing financial interests or personal relationships that could have appeared to influence the work reported in this paper.

Acknowledgements

The authors extend their appreciation to the Researchers Supporting Project number (RSPD2024R971), King Saud University, Riyadh, Saudi Arabia for funding this research.

References

[1] E. Moine, C. Denevault-Sabourin, F. Debierre-Grockiego, L. Silpa, O. Gorgette, J.C. Barale, et al., A small-molecule cell-based screen led to the identification of biphenylimidazoazines with highly potent and broad-spectrum anti-apicomplexan activity, Eur. J. Med. Chem. 89 (2015) 386–400, https://doi.org/10.1016/j.ejmech.2014.10.057.
[2] K.T. Andrews, G. Fisher, T.S. Skinner-Adams, Drug repurposing and human parasitic protozoan diseases, Inter. J. Parasito. Drug. Resis. 4 (2) (2014) 95–111, https://doi.org/10.1016/j.ijpddr.2014.02.002.
[3] S. Cikrikci, E. Mozioglu, H. Yilmaz, Biological activity of curcuminoids isolated from Curcuma longa, Record Nat. Prod. 2 (1) (2008) 19, https://doi.org/10.1590/S0074-02762001000500026.
[4] B. Whalström, G. Blennow, A study on the fate of curcumin in the rat, Acta Pharmacol. Toxicol. 43 (1978) 86–92, https://doi.org/10.1111/j.1600-0773.1978.tb02240.x.
[5] V. Ravindranath, N. Chandrasekhara, Absorption and tissue distribution of curcumin in rats, Toxicology 16 (3) (1980) 259–265, https://doi.org/10.1016/0300-483X(80)90122-5.
[6] E. Yuriev, P.A. Ramsland, Latest developments in molecular docking: 2010–2011 in review, J. Mol. Recogn. 26 (5) (2013) 215–239, https://doi.org/10.1002/jmr.2266.
[7] C. Mura, C.E. McAnany, An introduction to biomolecular simulations and docking, Mol. Simulat. 40 (10–11) (2014) 732–764, https://doi.org/10.1080/08927022.2014.935372.
[8] A.A. Tantar, S. Conilleau, B. Parent, N. Melab, L. Brillet, S. Roy, D. Horvath, Docking and biomolecular simulations on computer Grids, Curr. Comput. Aided Drug Des. 4 (3) (2008) 235–249, https://doi.org/10.2174/157340908785747438.
[9] O. Trott, A.J. Olson, AutoDock Vina: Improving the speed and accuracy of docking with a new scoring function, efficient optimization, and multithreading, J. Comput. Chem. 31 (2010) 455–461, https://doi.org/10.1002/jcc.21334.
[10] M. Rarey, B. Kramer, T. Lengauer, G. Klebe, A fast flexible docking method using an incremental construction algorithm, J. molecular biology. 261 (3) (1996) 470–489, https://doi.org/10.1006/jmbi.1996.0477.
[11] G.M. Morris, R. Huey, W. Lindstrom, M.F. Sanner, R.K. Belew, D.S. Goodsell, A.J. Olson, AutoDock4 and AutoDockTools 4: automated docking with selective receptor flexibility, J. computa. Chemi. 30 (16) (2009) 2785–2791, https://doi.org/10.1002/jcc.21256.
[12] G. Jones, P. Willett, R.C. Glen, A.R. Leach, R. Taylor, Development and validation of a genetic algorithm for flexible docking, J. Mol. Biol. 267 (3) (1997) 727–748, https://doi.org/10.1006/jmbi.1996.0897.
[13] T. Singh, D. Biswas, B. Jayaram, AADS-An automated active site identification, docking, and scoring protocol for protein targets based on physicochemical descriptors, J. Chem. Informat. Model. 51 (10) (2011) 2515–2527, https://doi.org/10.1021/ci200193z.
[14] R.B. Jacob, T. Andersen, O.M. McDougal, Accessible high-Throughput virtual screening molecular docking software for Students and Educators, PLoS Comput. Biol. 8 (2012) e1002499, https://doi.org/10.1371/journal.pcbi.1002499.
[15] Y. Fukunishi, Structural Rensemble in computational drug screening, Expet Opin. Drug Metabol. Toxicol. 6 (2010) 835–849, https://doi.org/10.1517/17425255.2010.486399.
[16] E. Kellenberger, J. Rodrigo, P. Muller, D. Rognan, Comparative evaluation of eight docking tools for docking and virtual screening accuracy, Proteins: Struct., Funct., Bioinf. 57 (2) (2004) 225–242, https://doi.org/10.1002/prot.20149.
[17] Damini Maithani, Anita Sharma, Saurabh Gangola, Parul Chaudhary, Pankaj Bhatt, Insights into applications and strategies for discovery of microbial bioactive metabolites, Microbiol. Res. 261 (2022) 127053, https://doi.org/10.1016/j.micres.2022.127053.
[18] L. Nuñez-Gonzalez, N. Carrera, M.A. Garcia-Gonzalez, Molecular basis, diagnostic challenges and therapeutic approaches of Bartter and Gitelman syndromes: a primer for Clinicians, Int. J. Mol. Sci. 22 (21) (2021) 11414, https://doi.org/10.3390/ijms222111414.
[19] J.M. Ribeiro, M.L. Rodrigues-Alves, E. Oliveira, P.P. Guimarães, A.M.M. Santi, A. Teixeira-Carvalho, et al., Pamidronate, a promising repositioning drug to treat leishmaniasis, displays antileishmanial and immunomodulatory potential, Int. Immunopharm. 110 (2022) 108952, https://doi.org/10.1016/j.intimp.2022.108952.
[20] H.A. Safdari, M.A. Ansari, F.B. Khan, A. Almatroudi, M.A. Alzohairy, M. Safdari, et al., Prospective therapeutic potential of Tanshinone IIA: an updated overview, Pharmacol. Res. 164 (2021) 105364, https://doi.org/10.1016/j.phrs.2020.105364.

[21] C.A. Nichol, G.K. Smith, D.S. Duch, Biosynthesis and metabolism of tetrahydrobiopterin and molybdopterin, Annu. Rev. Biochem. 54 (1) (1985) 729–764, https://doi.org/10.1146/annurev.bi.54.070185.003501.

[22] J. Wang, É. Leblanc, C.F. Chang, B. Papadopoulou, T. Bray, J.M. Whiteley, et al., Pterin and folate reduction by the Leishmania tarentolae H locus short-chain dehydrogenase/reductase PTR1, Arch. Biochem. Biophys. 342 (2) (1997) 197–202, https://doi.org/10.1006/abbi.1997.0126.

[23] A.R. Bello, B. Nare, D. Freedman, L. Hardy, S.M. Beverley, PTR1: a reductase mediating salvage of oxidized pteridines and methotrexate resistance in the protozoan parasite *Leishmania* major, Proc. Natl. Acad. Sci. USA 91 (24) (1994) 11442–11446, https://doi.org/10.1073/pnas.91.24.11442.

[24] R. Kumar, R.A. Bumb, N.A. Ansari, R.D. Mehta, P. Salotra, Cutaneous leishmaniasis caused by *Leishmania tropica* in Bikaner, India: parasite identification and characterization using molecular and immunologic tools, Am. J. Trop. Med. Hyg. 76 (2007) 896–901, https://doi.org/10.4269/ajtmh.12-0558.

[25] P. Kumar, A. Kumar, S.S. Verma, N. Dwivedi, N. Singh, M.I. Siddiqi, *Leishmania donovani* pteridine reductase 1: biochemical properties and structure-modeling studies, Exp. Parasitol. 120 (1) (2008) 73–79, https://doi.org/10.1016/j.exppara.2008.05.005.

[26] B. Nare, L.W. Hardy, S.M. Beverley, The roles of pteridine reductase 1 and dihydrofolate reductase-thymidylate synthase in pteridine metabolism in the protozoan parasite *Leishmania major*, J. Biol. Chem. 272 (1997) 13883–13891, https://doi.org/10.1074/jbc.272.21.13883.

[27] J. Wang, E. Leblanc, C.F. Chang, B. Papadopoulou, T. Bray, J.M. Whiteley, Pterin and folate reduction by the *Leishmania tarentolae* H locus short-chain dehydrogenase/reductase PTR1, Arch. Biochem. Biophys. 342 (1997) 197–202, https://doi.org/10.1006/abbi.1997.0126.

[28] A.R. Bello, B. Nare, D. Freedman, L. Hardy, S.M. Beverley, PTR1: a reductase mediating salvage of oxidized pteridines and methotrexate resistance in the protozoan parasite *Leishmania major*, in: Proceedings of the National Academy of Sciences of the United States of America, vol. 91, 1994, pp. 11442–11446, https://doi.org/10.1073/pnas.91.24.1144.

[29] M.L. Cunningham, S.M. Beverley, Pteridine salvage throughout the *Leishmania* infectious cycle: implications for antifolate chemotherapy, Mol. Biochem. Parasitol. 113 (2001) 199–213, https://doi.org/10.1016/S0166-6851(01)00213-4.

[30] A. Boakye, E.N. Gasu, J.O. Mensah, L.S. Borquaye, Computational studies on potential small molecule inhibitors of *Leishmania* pteridine reductase 1, J. Biomol. Struct. Dynam. (2023) 1–14, https://doi.org/10.1080/07391102.2023.2166119.

[31] Ina Pohner, Antonio Quotadamo, Joanna Panecka-Hofman, Rosaria Luciani, Matteo Santucci, Pasquale Linciano, Giacomo Landi, et al., Multitarget, selective compound design yields potent inhibitors of a kinetoplastid pteridine reductase 1, J. Med. Chem. 65 (13) (2022) 9011–9033, https://doi.org/10.1021/acs.jmedchem.2c00232.

[32] J.C. Contreras Esquivel, C.E. Voget, Purification and partial characterization of an acidic polygalacturonase from *Aspergillus kawachii*, J. Biotechnol. 110 (1) (2004) 21–28, https://doi.org/10.1016/j.jbiotec.2004.01.010.

[33] A.W. Sousa da Silva, W.F. Vranken, Acpype - AnteChamber PYthon Parser interfacE, BMC Res. Notes 5 (2012) 367. http://www.biomedcentral.com/1756-0500/5/367.

[34] D.E. Pires, T.L. Blundell, D.B. Ascher, pkCSM: predicting small-molecule pharmacokinetic and toxicity properties using graph-based signatures, J. Med. Chem. 58 (9) (2015) 4066–4072, https://doi.org/10.1021/acs.jmedchem.5b00104.

[35] J.G.M. Mvondo, A. Matondo, D.T. Mawete, S.M.N. Bambi, B.M. Mbala, P.O. Lohohola, *In silico* ADME/T properties of Quinine derivatives using SwissADME and pkCSM webservers, Int. J. Trop. Dis. Health 42 (2021) 1–12, https://doi.org/10.9734/ijtdh/2021/v42i1130492. IJTDH.71544.

[36] N.M. Cerqueira, D. Gesto, E.F. Oliveira, D. Santos-Martins, N.F. Brás, S.F. Sousa, P.A. Fernandes, M.J. Ramos, Receptor-based virtual screening protocol for drug discovery, Arch. Biochem. Biophys. 582 (2015) 56–67, https://doi.org/10.1016/j.abb.2015.05.011.

[37] Bernard R. Brooks, Robert E. Bruccoleri, Barry D. Olafson, David J. States, S.A. Swaminathan, Karplus Martin, CHARMM: a program for macromolecular energy, minimization, and dynamics calculations, J. Comput. Chem. 4 (2) (1983) 187–217, https://doi.org/10.1002/jcc.540040211.

[38] M.R.F. Pratama, H. Poerwono, S. Siswodiharjo, ADMET properties of 5 novel 5 Obenzoylpinostrobin derivatives, J. Basic Clin. Physiol. Pharmacol. (2019) 20190251, https://doi.org/10.1515/jbcpp-2019-0251.

[39] F. Bahrami, N. Masoudzadeh, S. Van Veen, J. Persson, A. Lari, H. Sarvnaz, Blood transcriptional profiles distinguish different clinical stages of cutaneous leishmaniasis in humans, Mol. Immunol. 149 (2011) 165–173, https://doi.org/10.1016/j.molimm.2022.07.008.

[40] A. Hosseini, F. Jaffary, G.R. Asghari, S.H. Hejazi, L. Shirani Bidabadi, *In vitro* effects of turmeric and licorice total extracts on *L. major* promastigotes, J. Isfahan Med. Sch. 29 (2012) 1–11.

[41] N. Tiwari, V. Kumar, M.R. Gedda, A.K. Singh, V.K. Singh, S.P. Singh, R.K. Singh, Identification and characterization of miRNAs in response to *Leishmania donovani* infection: delineation of their roles in macrophage dysfunction, Front. Microbiol. 8 (2012) 314, https://doi.org/10.3389/fmicb.2017.00314.

[42] N. Aara, K. Khandelwal, R.A. Bumb, D.R. Mehta, C.B. Ghiya, R. Jakhar, C. Dodd, P. Salotra, A.R. Satoskar, Clinco-epidemiologic study of cutaneous leishmaniasis in Bikaner, Rajasthan, India Naushin, Am. J. Trop. Med. Hyg. 89 (1) (2013) 111–115.

[43] A.C. Ivens, C.S. Peacock, E.A. Worthey, L. Murphy, G. Aggarwal, M. Berriman, et al., The genome of the kinetoplastid parasite, *Leishmania major*, Science 309 (5733) (2005) 436–442, https://doi.org/10.4269/ajtmh.12-0558.

[44] K. Kaur, T. Coons, K. Emmett, B. Ullman, Methotrexate-resistant Leishmania donovani genetically deficient in the folate-methotrexate transporter, J. Biol. Chem. 263 (15) (1988) 7020–7028, https://doi.org/10.1016/S0021-9258(18)68598-9.

[45] B. Thöny, G. Auerbach, N. Blau, Tetrahydrobiopterin biosynthesis, regeneration and functions, Biochem. J. 347 (1) (2000) 1–16, https://doi.org/10.1042/bj3470001.

[46] B. Nare, L.W. Hardy, S.M. Beverley, The roles of pteridine reductase 1 and dihydrofolate reductase-thymidylate synthase in pteridine metabolism in the protozoan parasite *Leishmania major*, J. Biol. Chem. 272 (21) (1997) 13883–13891, https://doi.org/10.1074/jbc.272.21.13883.

[47] D.G. Gourley, A.K. Shrive, I. Polikarpov, T. Krell, J.R. Coggins, A.R. Hawkins, et al., The two types of 3-dehydroquinase have distinct structures but catalyze the same overall reaction, Nat. Struct. Biol. 6 (6) (1997) 521–525.

[48] A.D. Knighton, G.C. Nanson, Flow transmission along an arid zone anastomosing river, Cooper Creek, Australia, Hydrol. Process. 8 (2) (1994) 137–154, https://doi.org/10.1002/hyp.3360080205.

[49] H.M. Kumalo, S. Bhakat, M.E. Soliman, Theory and applications of covalent docking in drug discovery: merits and pitfalls, Molecules 20 (2) (2015) 1984–2000, https://doi.org/10.3390/molecules20021984.